Interaction of a premixed flame with a liquid fuel film on a wall

Desoutter G.[1], Cuenot B.[1], Habchi C.[2] and Poinsot T.[3]

November 27, 2003

[1]CERFACS, 42 Avenue Coriolis

31057 TOULOUSE CEDEX FRANCE

[2]Institut Francais du Pétrole, 1 et 4 av du Bois Préau

92852 RUEIL MALMAISON FRANCE

[3]Institut de Mécanique des Fluides de Toulouse, Avenue C. Soula

31400 TOULOUSE FRANCE

Corresponding author:

Dr Bénédicte Cuenot

CERFACS - 42 Avenue Coriolis

31057 TOULOUSE CEDEX FRANCE

FAX: 33 5 61 19 30 00 - EMAIL: cuenot@cerfacs.fr

Colloqium: 10. Propulsion and Engine Combustion

Short title: Liquid film / flame interaction

Total length of paper: 4300 words (equations counted separately)

Listing of word count: Main text (2900) Equations (250) References (250) Figures (1:60, 2:60, 3:110, 4:140, 5:120, 6:150, 7:110, 8:140)

Abstract

In piston engines and in gas turbines, the injection of liquid fuel often leads to the formation of a liquid film on the combustor wall. If a flame reaches this zone, undesired phenomena such as coking may occur and diminish the lifetime of the engine. Moreover, the effect of such an interaction on maximum wall heat fluxes, flame quenching and pollutant formation is largely unknown. This paper presents a numerical study of the interaction of a premixed flame with a cold wall covered with a film of liquid fuel. Simulations show that the presence of the film leads to a very rich zone at the wall in which the flame cannot propagate. As a result, the flame wall distance remains larger with liquid fuel than it is for a dry wall and maximum heat fluxes are smaller. The nature of the interaction of flame wall interaction with a liquid fuel is also different from the classical flame / dry wall interaction: it is controlled mainly by chemical mechanisms and not by the thermal quenching effect observed for flames interacting with dry walls: the existence od a very rich zone created above the liquid film is the main mechanism controlling quenching.

Keywords: IC-Models, gas turbines, laminar flames, two-phase flames

1 Introduction

The interaction between walls and flames is a critical issue in the design of many modern combustion systems: in gas turbines, Lean Premixed Prevaporized (LPP) technologies often lead to the coexistence of liquid films on combustor walls and of flames (for example during flashback). In piston engines, Direct Injection (DI) techniques can create fuel films on the piston or on the cylinder walls: these films burn at later times, interacting with the flame in a complex manner which is not understood or modelled at the present time. This interaction may have several consequences on the flame and on the engine performance:

- the heat loss corresponding to the heat transfer from the flame to the liquid film may lead to local flame extinction, contributing to the production of unburnt hydrocarbons in the gas phase,
- the liquid fuel may not be totally evaporated and burned during a cycle, adding unburnt hydrocarbons at later times,
- the heat flux to the film may be transferred to the wall, damaging the wall and reducing performance,
- the liquid fuel may also burn on the wall, leading to coking phenomena on the chamber wall.

All these mechanisms are key problems for the emission of pollutant species and for the performance and the life time of the engine. They have to be taken into account in the design process of combustion chambers and require the development of new models for near-wall region. Studying the interaction of a flame with a wall covered with liquid fuel is therefore an interesting task both from the fundamental and the practical points of view.

Flame / wall interactions on dry walls (FWI-D) have been studied in premixed flames theoretically [1], experimentally [2,3] and numerically, both for laminar [4,5,6] and turbulent flows [7,8]. In these studies a generic FWI-D case is considered for laminar premixed flames (Fig. 1): the premixed flame propagates towards the wall and quenching is observed; the flame stops at a certain distance y_Q of the wall (of the order of the flame thickness) and the maximum wall flux Φ_Q^p (reached when the flame quenches) is of the order of one third of the total flame power $q = \rho_1 s_L^0 C_p(T_2 - T_1)$ where ρ_1 is the fresh gas density, s_L^0 is the flame speed and $C_p(T_2 - T_1)$ is the enthalpy jump through the flame [5].

In the present study, the basic configuration for the interaction of a flame with a wall covered with liquid fuel (FWI-LF) is displayed in Fig. 2. It is a simplified case in which the wall temperature is initially equal to the liquid film temperature and to the temperature of the fresh premixed gases. The initial thickness of the liquid film $h(t = 0)$ is one of the problem free parameters. The typical range of interest in engines is $10\mu m < h < 50\mu m$. Even though many other cases may occur in a turbulent combustor, this configuration is the simplest one and the logical choice to begin an investigation of FWI-LF mechanisms.

Although FWI-D is rather well understood in premixed [4,7] or diffusion flames [6] on dry walls, the introduction of a liquid film on the wall modifies the physics significantly. Before starting a detailed study, it is useful to evaluate some global characteristics of the processes involved. First, a simple estimate of the energy E_{ev} required to evaporate a liquid film of thickness h may be written as:

$$E_{ev} = Sh\rho_l L_v \tag{1}$$

where S is the film surface, ρ_l is the liquid density and L_v is the latent heat of vaporization. Thie energy may be compared to the total energy which can be delivered by a planar flame during its interaction with a cold wall, given by [1]:

$$E_{fl} = Sqt_f \tag{2}$$

In the above expression the duration of the interaction, that ends at flame quenching, is estimated by the flame time $t_f = D_{th}/s_L^0$ with D_{th} the thermal diffusivity in the fresh gas. Taking typical valiues of parameters (atmospheric

pressure, stoichioimetric hydrocarbon-air flame with fresh gases at $300K$), these two energies are found equal for a critical value of the film thickness $h_c = 1\mu m$. This shows that most films found in practice will not totally evaporate during their interaction with a flame. They will actually maintain their shape and only slightly reduce their thickness, so that assuming one-dimensionality for such a problem makes senses.

Under such an approximation, Fig. 3 proposes a simple scenario for a flame wall interaction in the case of Fig. 2. The computation begins at $t = 0$ with an isothermal liquid film and fresh gases at the same temperature. Rapidly ($t = t_1$), the evaporation process at the liquid gas interface ($y = 0$) leads to a decrease of the local temperature and the propagation of a temperature perturbation to the left in the liquid film (over a distance d named the penetration length), and to the right in the premixed gas. At the same time, the evaporation of the liquid film increases the fuel mass fraction in the fresh gases, generating a richer zone between the film surface and the flame. At the flame surface ($y = 0$), the fuel mass fraction always remains at the saturation value. At later times ($t = t_2$), the flame propagates and interacts with this richer zone. The simulations presented in the following sections quantify the scenario described above and in Fig. 3.

2 Numerical tool for FWI-LF

The problem of FWI-LF is a dual problem in which the temperature profile must be solved simultaneously in the gas and in the liquid film. As the liquid film contains fuel only, the species equations are solved only in the gas phase. The saturation Clausius-Clapeyron relations are used at the gas-liquid interface.

In the gas, a Direct Numerical Simulation code using a sixth-order compact scheme for spatial differencing and a third-order Runge Kutta scheme for time-advancement is used to compute the species mass fractions, the density and the temperature [4,9].

For the present study, a single-step reaction $Fuel + sOx \rightarrow Products$ (in mass) is sufficient (extensions to complex chemical schemes and surface catalysis effects are possible [10,11] but were not activated for this study). Boundary conditions are setup using the NSCBC technique [12]. The fuel reaction rate is expressed as:

$$\dot{\omega} = -A\rho^{n_f+n_o} Y_f^{n_f} Y_o^{n_o} exp\left(-\frac{T_a}{T}\right) \tag{3}$$

where the reaction exponents n_f and n_o are 0.65 and 3. The activation temperature is $15083K$. The stoichiometric ratio

s is 3.52. During the film evaporation the local equivalence ratio moves towards rich values. It is known that single step schemes cannot reproduce the flame speed decrease on the rich side. A simple solution is to use a variable pre-exponential factor A to match the flame speed variation for rich mixtures: A is taken as a function of the equivalence ratio, fitted on the s_L^0 curve of a typical hydrocarbon-air flame.

For the resolution of the temperature field in the liquid film, an integral method is used in which the temperature profiles are assumed to be polynomial functions of the spatial coordinate y. A comparison between the flame time t_f and the characteristic time of heat penetration in the film $t_w = h^2/D_{th}$ shows that heat conduction in the film is a slow process compared to the flame. Therefore two successive phases must be distinguished in the evolution of the temperature profile in the liquid film. Phase I corresponds to the penetration of heat in the liquid film, and lasts until the penetration depth $d(t)$ is equal to the film thickness $h(t)$. It is followed by phase II, in which heat conduction is present over the whole film thickness. Using adequate boundary conditions, and assuming that the wall ($y = h(t)$) is always covered by liquid at a constant temperature (T_w), the following form for the temperature profile in the liquid phase is obtained:

$$T(y,t) = T_w + \frac{1}{3\lambda_l}\left(2\phi_l(t)d(t) - 3\phi_l(t)y + \phi_l(t)\frac{y^3}{d(t)^2}\right) \tag{4}$$

where $\phi_l(t)$ is the heat flux through the film surface at $y = 0$. The penetration depth $d(t)$ is the solution of:

$$\frac{d}{dt}\left(\phi_l(t)d(t)^2\right) = 4\frac{\lambda_l}{\rho_l C p_l}\phi_l(t) \tag{5}$$

This expression holds for $y = 0$, giving the film surface temperature T_s:

$$T_s = T_w + \frac{2\phi_l(t)d(t)}{3\lambda_l} \tag{6}$$

In Phase II, starting as soon as the penetration depth $d(t)$ reaches $h(t)$, the boundary conditions change and a different polynomial approximation must be used:

$$T(y,t) = T_w - \frac{h(t)-y}{2h(t)\lambda_l}\left[3(T_w - T_s)\lambda_l + h(t)\phi_l(t) + ((T_w - T_s)\lambda_l + h(t)\phi_l(t))\left(1 - \frac{y}{h(t)}\right)^2\right] \tag{7}$$

with T_s solution of:

$$\frac{d}{dt}\left(-\frac{\phi_l(t)h(t)}{\lambda_l} + 5T_s\right) = \frac{12}{\rho_l C p_l h^2(t)}\left(\lambda_l(T_w - T_s) + \phi_l(t)h(t)\right) \tag{8}$$

The heat flux $\phi_l(t)$ is known from the heat flux in the gas phase and the evaporation mass flux $\dot{M}$:

$$\phi_l(t) = \phi_g(t) + \dot{M}L_v \tag{9}$$

Finally, the film thickness obeys:

$$\frac{dh(t)}{dt} = -\frac{\dot{M}}{\rho_l} \tag{10}$$

At the liquid / gas interface ($y = 0$), the Clausius-Clapeyron relation is supposed to hold at all times, allowing to calculate $\dot{M}$ from the saturation conditions.

3 FWI-D reference case: the premixed flame on a dry wall

First, the case of a premixed flame with an equivalence ratio of 0.8 interacting with a dry wall at fixed temperature ($T_w = 300K$) is computed as a reference case. The maximum heat flux Φ_Q^p measured during this interaction is used as the reference value to scale all cases. Fig. 4 shows the flame / wall distance, the flame consumption speed and the wall heat flux versus time. All values are normalized: the flame / wall distance y is scaled by the flame thickness $\delta = D_{th}/s_L^0$, the flame consumption speed s_c (obtained by $s_c = -\int \dot{\omega}_F dx/\rho_1 Y_{F,1}$ where $\dot{\omega}_F$ is the fuel reaction rate) is normalized by the unstrained planar flame speed s_L^0 and the wall heat flux ϕ_w is scaled by the flame power q. Before the interaction starts, the flame-wall distance decreases linearly indicating that the flame moves at constant speed s_L^0. It then slows down and stops when $y/\delta = y_Q/\delta \simeq 3.46$. At this moment, the normalized heat flux ϕ_Q^p/q is maximum, of the order of 0.40. Both observations are consistent with previous experimental and numerical work [5].

4 FWI-LF: interaction of a flame with a wall covered by a liquid film

This section describes numerical results in the case of a wall at $T_w = 300K$ covered by a film of initial thickness $h = 20\mu m$ interacting with a laminar premixed flame (same flame as in section 3). The mean pressure is 1 bar. Fig. 5 and 6 show profiles of the temperature and fuel mass fraction at different times from $t = 0ms$ to $t = 21.3ms$. For temperature, a zoom shows the detail of the profiles in the liquid film.

The fuel evaporation at the film surface results first in a small decrease of the temperature at this point (down to $\approx 298K$), then heat conduction brings T_s back to the wall temperature $T_w = 300K$. Eventually the presence of hot gas at the film surface raises the interface temperature. Phase I ends at $t = 0.7ms$, when $d(t) = h(t)$. Fig. 7 shows the time evolution of the film thickness $h(t)$. The fuel evaporates during this interaction but its thickness $h(t)$ changes only from 20μm at $t = 0$ to 19.4μm after the flame quenching. This is consistent with the film thickness estimation given in

section 1.

In the gas, the temperature profiles show the flame approaching the film, being perturbed and quenched, and propagating back. This scenario is quite similar to the flame interaction with a dry wall, with however two important differences:

- while the flame approaches the film, the maximum temperature increases, indicating an increasing equivalence ratio,
- the flame quenches before reaching the film surface, i.e. without significant heat transfer to the liquid film and the wall.

The increased temperature and flame speed during the flame propagation towards the film are explained by the fuel vapor release due to evaporation. Starting from 0.8 initially, the equivalence ratio in front of the flame becomes closer to stoichiometry, enhancing combustion and resulting in higher temperatures. This is illustrated on the mass fraction profiles of Fig. 6: after $t \approx 8ms$, the fuel mass fraction in the fresh gas in front of the flame increases, and rapidly goes over the stoichiometric value ($Y_{F,st} = 0.067$). As the film surface temperature T_s varies very little the fuel mass fraction saturation value $Y_{F,S}$ at the liquid/gas interface is quasi constant at the value 0.43, far above the stoichiometric value.

The evolution of the equivalence ratio "seen" by the flame depends on the initial flame distance from the liquid film. When the flame starts far from the film, the fuel mass fraction diffuses for a long time before meeting the flame and the spatial variation of the fuel mass fraction is smooth. Starting the flame closer to the film results in an increased slope of the fuel mass fraction profile and a more rapidly changing equivalence ratio. In the present case the initial distance between the wall and the flame is approximately 80 times the flame thickness.

This change of equivalence ratio is the key point of the flame/liquid film interaction. Looking at the mass fraction profiles, it can be expected that the flame will reach its rich flammability limit while still quite far from the film surface, i.e. before significant heat transfer to the liquid phase takes place. This means that the flame quenching is not due to heat loss, a fundamental difference with the case of the interaction with a dry wall. The flame quenching is due here to the rich fresh gas mixture generated by the film evaporation, i.e. to a chemical effect. The main consequence is a long quenching distance and a very small heat flux to the film and the wall. This is illustrated on Fig. 8, showing the scaled flame/film distance (y/δ), the scaled flame speed (s_c/s_L^0) and the heat flux to the liquid film normalized by the reference value Φ_Q^p (ϕ_l/Φ_Q^p).

Four important observations can be made:

- the minimum reduced flame distance to the film y/δ is 20, much higher than the quenching distance $y_Q = 3.5$ of the flame interacting with a dry wall. This is due to the fact that the flame quenching is controlled by chemistry and not heat loss. This minimum distance changes with the initial flame/film distance, as this distance has an effect on the location of the rich flammability limit. However, the mass fraction value corresponding to the rich flammability limit ($Y_F \approx 0.1$) being much smaller than the saturation value found at the film surface, the quenching point is always higher than the reference distance y_Q,

- the flame consumption speed increases when the flame starts to burn the evaporated fuel (around $7.5ms$), then drops abruptly when the rich flammability limit is reached, with a maximum at $9.5ms$ (corresponding to the minimal flame/film distance). This drop corresponds to the flame extinction, completed at $t = 11ms$,

- the heat flux at the liquid/gas interface is first controlled by the heat diffusion in the liquid film. It then comes back to zero and remains null during the flame acceleration and extinction. Finally it starts to raise only after $12ms$, when hot gases arrive at the film surface and remains always much lower than the reference value Φ_Q^p obtained on a dry wall, with a time increase rate smaller by two orders of magnitude than in the case of interaction with a dry wall. This indicates that the flame has no influence on the heat flux to the film and the wall, mainly due to the presence of hot gases at the film surface,

- finally, since the heat flux to the film is much smaller than it is on a dry wall, the film is actually "isolated" from the flame effects by its own vapor. The film does not evaporate and it stays on the wall. This is an important point to evaluate the life time of liquid fuels and their possible contribution to the emission of unburnt hydrocarbons.

5 Conclusions

This work shows that the presence of a liquid film on a wall strongly modifies the mechanisms of interaction between the wall and flame fronts. The evaporation of fuel at the liquid / gas interface leads to a very rich zone close to the film into which the flame cannot propagate. As a result, when the interaction of a premixed flame with a dry wall (FWI-D) is compared with the case of a flame interacting with a wall covered by a fuel film (FWI-LF), the flame quenches further away from the wall, as quenching is controlled by chemistry and not thermal losses, and the maximum heat

fluxes are much smaller. A direct consequence is that the fuel film evaporates only marginally during the interaction with the flame front.

6 References

1. I. Wichman, G. Bruneaux, *Combust. Flame* 103 (4) (1995) 296-310.

2. J. Jarosinski, *Combust. Sci. Tech.* 12 (1986) 81-116.

3. O. A. Ezekoye, R. Greif, R. F. Sawyer, *Proc. of the Combust. Inst.* 24 (1992) 1465-1472.

4. T. Poinsot, D. Haworth, G. Bruneaux, *Combust. Flame* 95 (1/2) (1993) 118-133.

5. T. Poinsot, D. Veynante, *Theoretical and numerical combustion*. R.T. Edwards, Inc. , USA, 2001.

6. A. Delataillade, F. Dabireau, B. Cuenot, T. Poinsot, *Proc. of the Combust. Inst.* 29 (2002) 775-780.

7. G. Bruneaux, K. Akselvoll, T. Poinsot, J. Ferziger, *Combust. Flame* 107 (1/2) (1996) 27-44.

8. T. Alshaalan, C.J. Rutland, *Proc. of the Combust. Inst.* 27 (1998) 793-799.

9. Cuenot, B. and Poinsot, T., *Proc. of the Combustion Institute* 25:((1994) 1383-1390.

10. P. Popp, M. Smooke, M. Baum, *Proc. of the Combust. Inst.* 26 (1996) 2693-2700.

11. P. Popp, M. Baum, *Combust. Flame* 108 (3) (1997) 327 - 348.

12. T. Poinsot, S. Lele,*J. Comput. Phys.* 101 (1) (1992) 104-129.

List of Figures

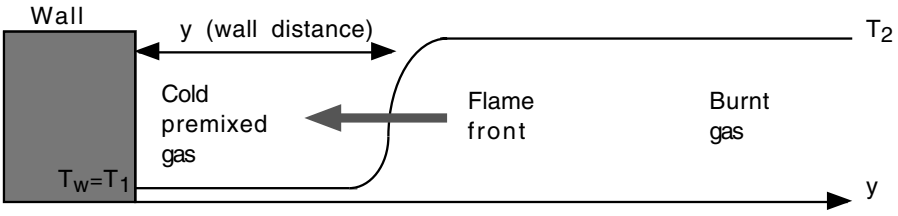

Figure 1: The basic configuration for flame/wall interaction in premixed flames.

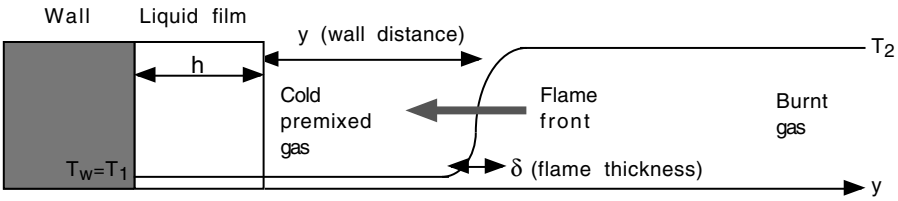

Figure 2: The basic configuration for flame/wall interaction with liquid film.

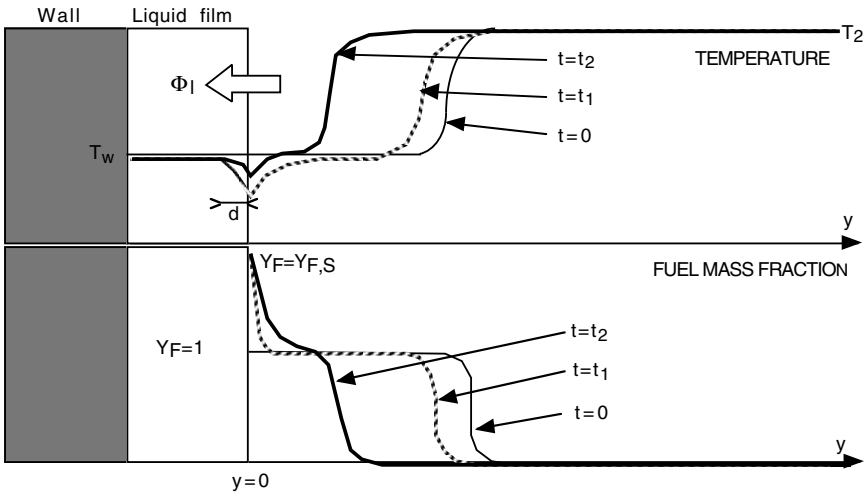

Figure 3: Illustration of the physics of flame wall interaction in the presence of a liquid film.

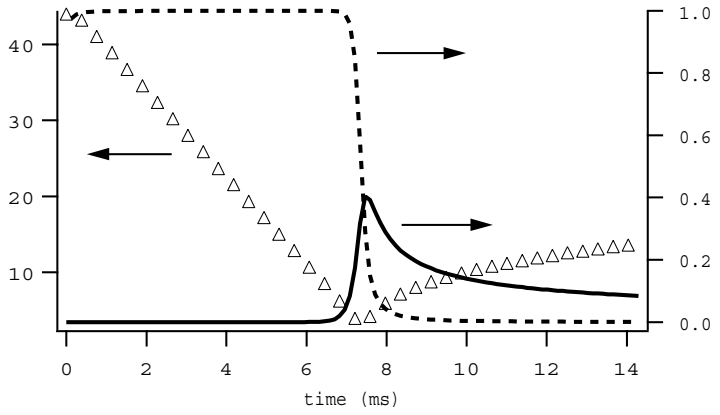

Figure 4: Normalized flame / wall distance y/δ (△), consumption speed s_c/s_L^0 (- - - -) and wall heat flux ϕ_w/q (———) during FWI for a premixed flame.

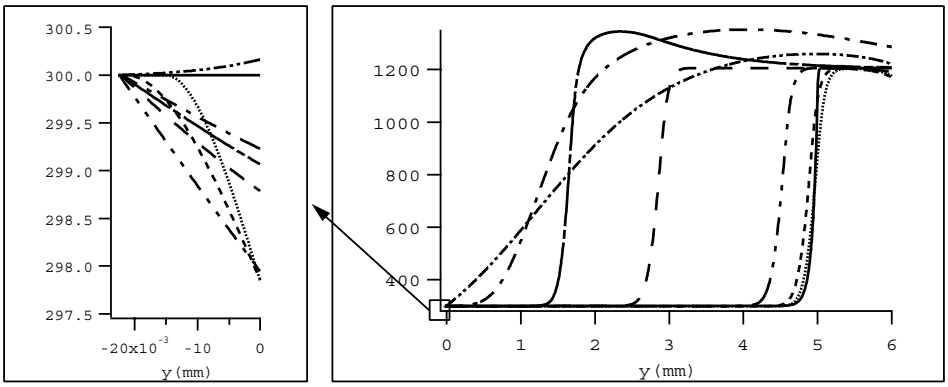

Figure 5: Temperature profiles at times $t = 0ms$ (———), $t = 0.29ms$ (·····), $t = 0.58ms$ (- - - -) for phase I, and $t = 1.73ms$ (— - -), $t = 6.9ms$ (——), $t = 10.34ms$ (——— -), $t = 13.8ms$ (— - —) and $t = 21.3ms$ (- ··) for phase II in FWI-LF.

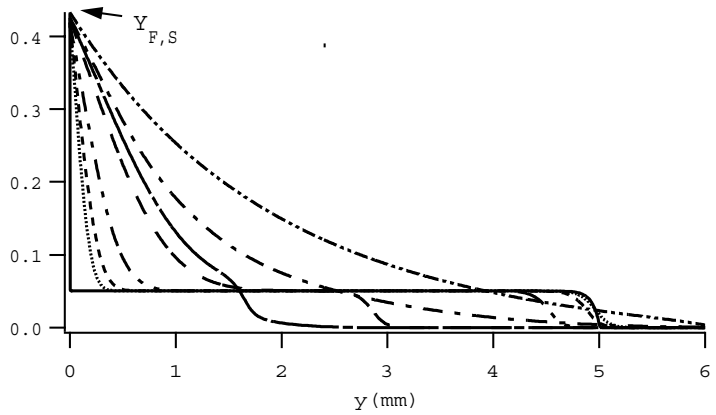

Figure 6: Fuel mass fraction profiles at times $t = 0ms$ (———), $t = 0.29ms$ (·····), $t = 0.58ms$ (- - - -) for phase I, and $t = 1.73ms$ (— - -), $t = 6.9ms$ (——), $t = 10.34ms$ (——— -), $t = 13.8ms$ (— - —) and $t = 21.3ms$ (- ··) for phase II in FWI-LF.

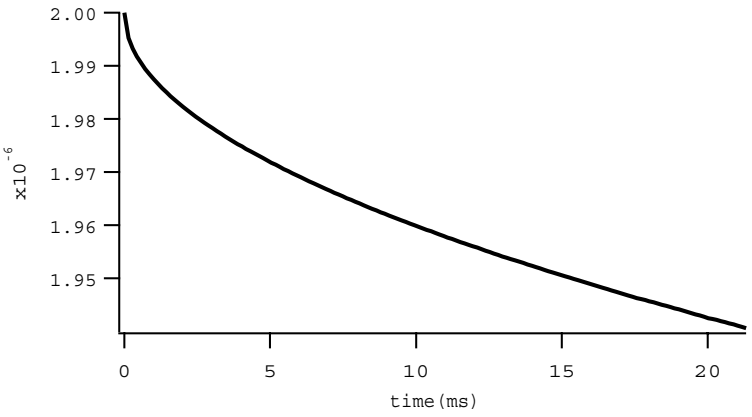

Figure 7: Time evolution of the liquid film thickness for FWI-LF.

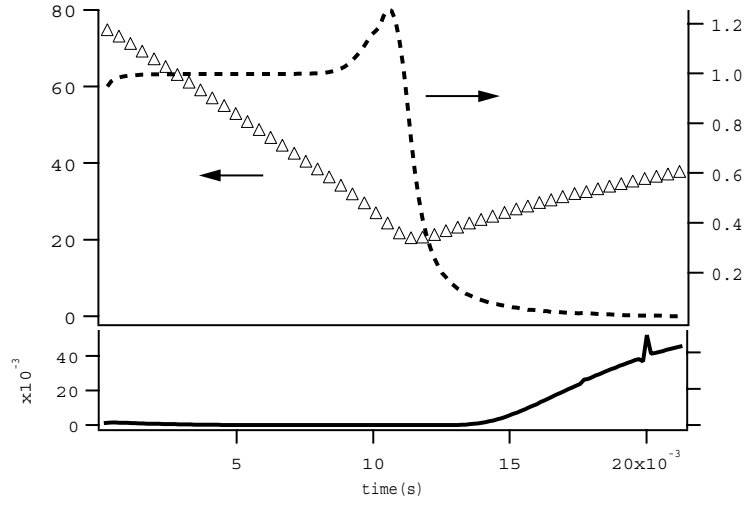

Figure 8: Normalized flame / wall distance y/δ ($\triangle$), consumption speed s_c/s_L^0 (- - - -) and wall heat flux ϕ_l/Φ_Q^p (———) during the flame interaction with a liquid film.